




# Prediction of vascular invasion using a 7-point scale computed tomography grading system in adrenal tumors in dogs

Pascaline Pey<sup>1,2</sup>  | Swan Specchi<sup>3†</sup> | Federica Rossi<sup>4†</sup> | Alessia Diana<sup>1</sup>  |  
 Ignazio Drudi<sup>5</sup> | Allison L. Zwingenberger<sup>6</sup> | Philipp D. Mayhew<sup>6</sup> |  
 Luciano Pisoni<sup>1</sup> | Daniele Mari<sup>7</sup> | Federico Massari<sup>3</sup> | Boris Dalpozzo<sup>4</sup> |  
 Federico Fracassi<sup>1</sup>  | Stefano Nicoli<sup>7†</sup>

<sup>1</sup>Department of Veterinary Medical Science, Alma Mater Studiorum, University of Bologna, Ozzano Emilia (BO), Italy

<sup>2</sup>Antech Imaging Services, Irvine, CA, USA

<sup>3</sup>Ospedale Veterinario i Portoni Rossi, Bologna (BO), Italy

<sup>4</sup>Clinica Veterinaria dell'Orologio, Sasso Marconi (BO), Italy

<sup>5</sup>Department of Statistical Sciences, Alma Mater Studiorum, University of Bologna, Bologna (BO), Italy

<sup>6</sup>Department of Surgical & Radiological Sciences, School of Veterinary Medicine, University of California, Davis, California, USA

<sup>7</sup>Clinica Veterinaria Roma Sud, Rome, Italy

## Correspondence

Pascaline Pey, Department of Veterinary Medical Science, Alma Mater Studiorum, University of Bologna, Ozzano Emilia (BO), Italy.  
 Email: pascaline\_vey@hotmail.fr

## Abstract

**Background:** Previous studies evaluating the accuracy of computed tomography (CT) in detecting caudal vena cava (CVC) invasion by adrenal tumors (AT) used a binary system and did not evaluate for other vessels.

**Objective:** Test a 7-point scale CT grading system for accuracy in predicting vascular invasion and for repeatability among radiologists. Build a decision tree based on CT criteria to predict tumor type.

**Methods:** Retrospective observational cross-sectional case study. Abdominal CT studies were analyzed by 3 radiologists using a 7-point CT grading scale for vascular invasion and by 1 radiologist for CT features of AT.

**Animals:** Dogs with AT that underwent adrenalectomy and had pre- and postcontrast CT.

**Results:** Ninety-one dogs; 45 adrenocortical carcinomas (50%), 36 pheochromocytomas (40%), 9 adrenocortical adenomas (10%) and 1 unknown tumor. Carcinoma and pheochromocytoma differed in pre- and postcontrast attenuation, contralateral adrenal size, tumor thrombus short- and long-axis, and tumor and thrombus mineralization. A decision tree was built based on these differences. Adenoma and malignant tumors differed in contour irregularity. Probability of vascular invasion was dependent on CT grading scale, and a large equivocal zone existed between 3 and 6 scores, lowering CT accuracy to detect vascular invasion. Radiologists' agreement for detecting abnormalities (evaluated by chance-corrected weighted kappa statistics) was excellent for CVC and good to moderate for other vessels. The quality of postcontrast CT study had a negative impact on radiologists' performance and agreement.

**Abbreviations:** AT, adrenal tumor; CT, computed tomography; CVC, caudal vena cava; DICOM, Digital Imaging and Communications in Medicine; DOR, diagnostic odds ratio; HU, Hounsfield unit; MPR, multiplanar reconstruction; PA, phrenicoabdominal; ROI, region-of-interest.

<sup>†</sup>These authors contributed equally.

This is an open access article under the terms of the Creative Commons Attribution-NonCommercial-NoDerivs License, which permits use and distribution in any medium, provided the original work is properly cited, the use is non-commercial and no modifications or adaptations are made.

© 2022 The Authors. *Journal of Veterinary Internal Medicine* published by Wiley Periodicals LLC on behalf of American College of Veterinary Internal Medicine.

**Conclusions and Clinical Importance:** Features of CT may help radiologists predict AT type and provide probabilistic information on vascular invasion.

**KEYWORDS**

canine, carcinoma, CT, pheochromocytoma, thrombus

## 1 | INTRODUCTION

The most frequent malignant adrenal tumors (ATs) in dogs are adrenocortical carcinoma and pheochromocytoma.<sup>1-3</sup> In this species, most malignant ATs spread by both the hematogenous and lymphatic routes.<sup>1</sup> However, they tend to spread early by direct invasion of surrounding structures, in particular, the adjacent veins.<sup>1</sup> Extension of the tumor into the phrenicoabdominal (PA) vein, renal vein or caudal vena cava (CVC) is not unusual in dogs.<sup>4-6</sup> This information is extremely important for the surgeon to gain vascular control during the adrenalectomy procedure<sup>5-12</sup> and choose the appropriate surgical technique (ie, open laparotomy, laparoscopic adrenalectomy, type of venotomy).<sup>13,14</sup> The presence, size and extent of the tumor thrombus also may have an impact on prognosis.<sup>6,10</sup> Major peri-operative complications include sudden death, respiratory arrest, acute kidney injury, hemorrhage, acute respiratory distress syndrome, regurgitation, pancreatitis, hypotension, and aspiration pneumonia. The peri-operative major complication rate varies from 11% for adrenalectomy for small ATs without vascular invasion<sup>12</sup> to 24% for invasive ATs treated by adrenalectomy and cavotomy, for experienced surgeons.<sup>11</sup> Preoperative knowledge of adjacent organ invasion, such as the kidney, is also crucial for the surgeon because concurrent nephrectomy has been associated with a guarded prognosis in some studies.<sup>8</sup>

Computed tomography (CT) is an accurate method for detection of vascular invasion by malignant ATs,<sup>15-19</sup> with reported sensitivity of 92% and specificity of 100%.<sup>15</sup> Furthermore, excellent agreement between CT and pathology for vascular invasion has been demonstrated.<sup>16</sup> In previous studies,<sup>15,16</sup> the CT reading method to detect vascular invasion was limited to the description of endoluminal thrombus with clear vascular invasion. However, the presence of streamlining artifacts and a delayed acquisition after contrast administration may increase the difficulty in thrombus assessment.<sup>17-19</sup> Some ATs, because of their large size, may be in contact with, compress, or occlude the adjacent vessels, making the diagnosis of vascular invasion extremely difficult. Because the perioperative complication rate is high, the use of improved preoperative CT technique and interpretation methods may be of value in more accurately determining tumor invasiveness. In human medicine, CT grading systems using point-scale methods have been developed to improve the accuracy and efficiency of the radiologist in predicting vascular invasion or infiltration of adjacent tissues as reported in patients affected by pancreatic ductal adenocarcinoma.<sup>20,21</sup> The grading system has been proven to have excellent agreement with surgery, histopathology and is well-correlated to prognosis.<sup>20,21</sup>

Because the preoperative treatment and surgical approach differ among AT types, knowing before surgery which tumor type is

involved (ie, adrenocortical adenoma, carcinoma, or pheochromocytoma) remains crucial.<sup>7,22</sup> Therefore, our objectives were to evaluate the agreement between a CT grading system and surgical exploration, the accuracy of the CT grading system in predicting vascular invasion, and the accuracy of CT criteria in predicting tumor type in patients with ATs. Furthermore, we aimed to evaluate the agreement among radiologists to test the repeatability of the CT grading system.

## 2 | MATERIALS AND METHODS

### 2.1 | Patient population

Dogs with AT were retrospectively enrolled in this multicenter study. Inclusion criteria were pre- and postcontrast abdominal CT, adrenalectomy within 1 week of the CT, and a detailed surgical report in the database. Presence of a histopathological report was not an inclusion criterion but was recorded if available. All identifiable data from the medical records (dog identification, institution, histopathological diagnosis, results of surgical report) was deidentified and randomized for evaluation.

### 2.2 | Image evaluation

The CT images were transferred to a workstation using commercially available Digital Imaging and Communications in Medicine (DICOM) imaging viewing software (Osirix MD v 9.0.1, Pixmeo SARL, Bernex, Switzerland). Each CT study was anonymized, deleting sensitive information from the metadata attached to the DICOM images. A single radiologist independently evaluated each AT and its CT features.

The following variables were evaluated: (a) dimensions of each AT obtained on multiplanar reconstruction (MPR) images: short axis (mm), long axis (mm); (b) mean attenuation value on pre- and postcontrast images (in Hounsfield units [HU]) using a region-of-interest (ROI) that was manually drawn over the maximal area of tumor parenchyma on transverse images (automatic circle), avoiding areas of mineralization when present; (c) type of enhancement (homogeneous, heterogeneous, presence of rim enhancement); (d) presence of mineral foci; (e) contours (smooth, irregular); (f) presence of hyperattenuating perirenal adipose tissue (yes or no); and, (g) presence of tumor rupture (yes or no). Tumor rupture was defined as tumor fracture or spillage with presence of peritumoral blood-attenuating fluid or material. The maximal thickness of the caudal pole of the contralateral adrenal gland also was recorded (in mm) using a previously described technique.<sup>23</sup>

When a tumor thrombus was present, the following imaging features were recorded: (a) dimensions obtained on postcontrast MPR images: short and long axes (mm), (b) presence of mineral foci within the tumor thrombus (yes or no), and (c) enhancement (homogeneous, heterogeneous). The long axis of the thrombus was measured as the length from the most cranial part to the base of the thrombus in its intracaval portion. The short axis was the maximal diameter of the tumor thrombus in the vessel, perpendicular to the long axis of the thrombus.

## 2.3 | Grading system

The grading process for vascular invasion by the tumor was performed by 3 radiologists. These 3 radiologists came from different clinical settings (academic vs private practice), were trained at different centers, and had variable clinical backgrounds. The radiologists' responses were anonymized, and they were blinded from all of the following variables: dog identity; surgical report; histopathological report; institution where the CT study was performed; brand, type, and number of slices of the CT scanner; and, results of the other 2 radiologists. A training session for the 3 radiologists was carried out before initiation to explain the CT grading system.

A 7-point CT grading system for evaluation of vascular invasion was used (Figure 1), inspired by a 3-point CT grading system used in human medicine to evaluate pancreatic ductal adenocarcinoma.<sup>20,21</sup> Grade 1 represents an absence of contact between the vessel and the mass as a layer of adipose tissue identified in between. Grade 2 shows contact between the 2 structures, affecting  $<90^\circ$  of the circumference of the vessel. Grade 3 represents contact affecting  $>90^\circ$  of the vessel with a concave aspect of the tumor, encircling the vessel. Grade 4 depicts increased contact between the structures, affecting  $>90^\circ$  of the vessel, with a convex aspect of the tumor against the vessel, the 2 structures having smooth regular margins. In grade 5, the tumor also has a convex aspect against the vessel, but the margins are irregular and ill-defined. Grade 6 represents compression of the vessel by the tumor, making it impossible to identify the contact point. Grade 7 describes clear invasion of the vessel by the tumor.

Each radiologist graded the point of contact between the tumor and the phrenicoabdominal (PA) vein, renal vein, CVC, aorta, and cranial mesenteric artery, using a scale of 1 to 7. For each of these structures, the radiologist was asked to select which of the MPR plane had been the most useful and pertinent to assess the grading of the point of contact between the AT and the vessel. When an arterial phase was available, the radiologist was asked to answer whether this phase was useful in predicting vascular invasion. The visualization of hyperattenuating tissue in the mesenteric lymphatic network (surrounding the cranial mesenteric and celiac artery roots) and presence of enhancement of this tissue at the level of the tumor was recorded.

## 2.4 | Image quality

Presence of artifacts and their type also were recorded. The usefulness of the arterial phase was evaluated by each radiologist for

evaluation of potential endothelial invasion by the thrombus, for evaluation of the margins of the tumor, for evaluation of the enhancement of the mesenteric lymphatic network and for evaluation of invasion of adjacent organs. Each radiologist could evaluate the quality of the CT study by providing a grade between 0 (insufficient) and 5 (excellent). Results then were exported to a spreadsheet opened using a dedicated program (Google sheet, Google LLC, Mountain View, California), where no information about the institutions, radiologists, clients, and dogs was present.

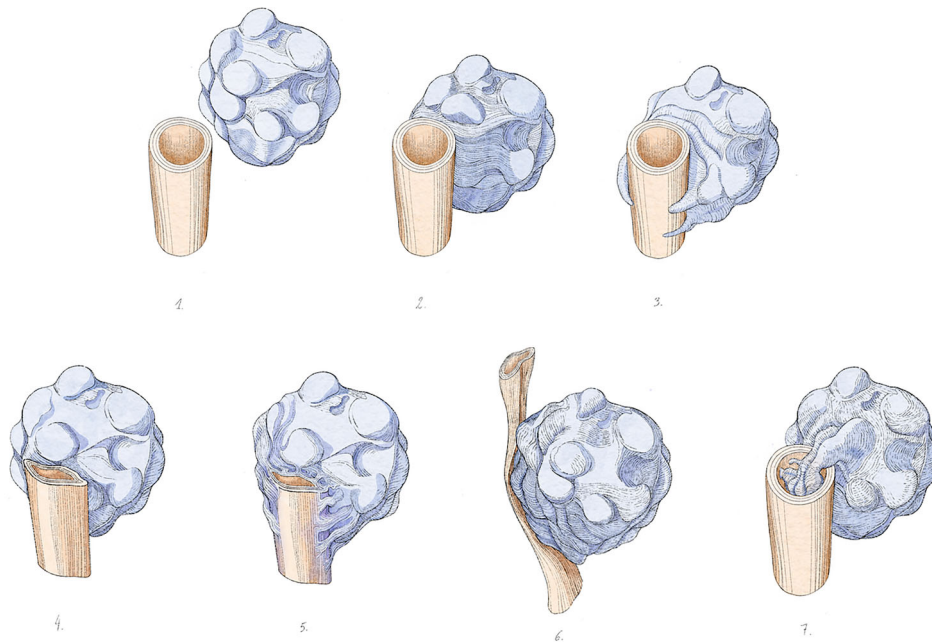
## 2.5 | Data analysis

Statistical analysis was performed using "R-4.0.5 for Windows" available under General Public license (R Core Team; 2013).<sup>24</sup> The differences in frequencies of CT criteria (described in the material and methods) between tumoral types were investigated. For variables showing a Gaussian distribution (according to the D'agostino and Pearson test), the parametric *t*-test was used, whereas the nonparametric Kolmogorov-Smirnoff test was applied for non-Gaussian variables. The level of significance was set at .05. A multivariable analysis of impact on the diagnoses of the entire set of variables was investigated.

A decision tree algorithm<sup>25</sup> was applied, identifying a threshold in the continuous variables (as precontrast attenuation values or long axis of thrombus) below and above which the probability of identifying the type of tumor became significantly lower or higher compared with the alternative diagnosis. In addition, the weight of the risk of misclassification with a cost function representing the (probabilistic) gain or loss associated with a wrong decision (ie, type I and type 2 errors) was evaluated.<sup>26</sup> A wrong decision or wrong diagnosis corresponded to a false decision or diagnosis compared to the final histopathological report, a disagreement between the radiologist's diagnosis and the final histopathological report. In addition to generating an easy guide for the radiologist's diagnoses to minimize the risk-cost function, a sequence of rules (type IF, THEN) was presented as supplementary output of the decision tree the output of which was not easily used.


The quality of results of the decision tree was closely correlated with the reliability of input data (ie, the diagnoses of the radiologists). The reliability of radiologist judgments was evaluated by calculating sensitivity, specificity, positive predictive value (PPV), negative predictive value (NPV), diagnostic odds ratio (DOR) and accuracy in predicting vascular invasion on CT compared with the surgical report for each radiologist and for selected vessels. Diagnostic odds ratio is a measure of the effectiveness of a diagnostic test. It is defined as the ratio of the odds of the test being positive if the subject has the disease relative to the odds of the test being positive if the subject does not have the disease. The interobserver agreement among radiologists for vascular invasion detection with the surgical report was calculated using chance-corrected weighted kappa ( $\kappa$ ) statistics:  $\kappa < 0.20$  was considered to indicate poor agreement,  $\kappa$  of 0.20 to 0.39 fair agreement,  $\kappa$  of 0.40 to 0.59 moderate agreement,  $\kappa$  of 0.60 to 0.79 good agreement, and  $\kappa \geq 0.80$  excellent


(A)
















(B)

### 7-point scale CT grading system

 = vessel

 = tumor

CRITERIA	GRADING		
No contact (presence of a layer of adipose tissue between the tumour and the vessel)	1		
Contact <90°, with smooth margins	2		
Contact >90°, concave aspect of the tumour (encircling the vessel)	3		
Contact >90°, convex aspect of the tumour against the vessel (mass effect) with smooth margins	4		
Contact: convex aspect of the tumor against the vessel (mass effect) with irregular margins	5		
Compression of the vessel, impossibility to visualize the point of contact or the vessel is not visible (maybe thrombosed?)	6		
Clear invasion	7		

**FIGURE 1** Illustration (A) and table (B) representing the grades of vascular invasion by the adrenal tumor

agreement. The level of significance was set at .05. Both linear and quadratic weight were used with no significant differences in the results.

To investigate the role of intermediate evaluation (ie, grades ranging from 3 to 6), the Bayes' theorem was followed to examine to what probabilistic extent the presence of a given grade was a

sign of the presence of invasion. In other words, we answered the question, "What is the probability of observing invasion of the CVC if a grade 3, or 4, 5, 6 (intermediate, uncertain answer) has been formulated by a radiologist?". Bayes' theorem is a powerful method for addressing so-called "inverse problems" by using evidence to

update the probability of each possible cause. In our study, the evidence was a given grade, and the cause was the presence or absence of invasion. The same Bayes' theorem was applied for mesenteric and aortic adherence (presence and enhancement of lymphatic network). In the above context, we referred to "pure Bayes' theorem," which is the correct formula to determine the conditional probability of a given cause, hence the framework is probability theory in its basic formulation, not classification procedures that are usual in expert systems, such as Bayesian learning or naïve Bayes classifier.

### 3 | RESULTS

#### 3.1 | Patient population

One-hundred dogs were recruited for the study. Nine cases were excluded because of incomplete CT studies or lack of a surgical report. From these 91 included cases, 90 had histopathological analysis available. They came from 6 different centers (2 university teaching hospitals and 4 private practices).

#### 3.2 | Tumor type and vascular invasion

There were 39 tumors involving the right adrenal gland (43%) and 52 involving the left (57%). There were 45 adrenocortical carcinomas (50%), 36 pheochromocytomas (40%) and 9 adrenocortical adenomas (10%). On surgery, we observed 37 tumor thrombi invading the CVC (40%); 22 originating from a pheochromocytoma (61%), 14 from an adrenocortical carcinoma (39%) and 1 from a tumor for which the histopathological analysis was not available. Six renal veins (by 3 adrenocortical carcinomas and 3 pheochromocytomas) and 43 PA veins (by 18 adrenocortical carcinomas, 24 pheochromocytomas and 1 from

the tumor for which the histopathological analysis was not available) were invaded.

At surgery, adherence was observed between 11 tumors and the aorta, and 24 tumors and the cranial mesenteric artery.

#### 3.3 | Morphologic and dimensional features

Adrenocortical carcinoma and pheochromocytoma differed in their pre- and postcontrast mean attenuation values, for the size of the contralateral AG, the short and long axes of the tumor thrombus when present, the presence of mineralization in the tumor, and in the thrombus (Table 1). In particular, pheochromocytoma had higher mean precontrast and postcontrast attenuation values compared to carcinoma. Pheochromocytoma had larger and longer tumor thrombus compared to carcinoma. Pheochromocytoma and the associated tumor thrombus were less frequently mineralized compared to carcinoma. Adrenocortical adenoma and carcinoma had lower mean size of contralateral adrenal gland compared to pheochromocytoma. Adrenocortical carcinoma and pheochromocytoma displayed irregular contours more frequently compared to adrenocortical adenoma.

Dimensions of the tumors and thrombi, contralateral AG, and attenuation values of the tumors are reported in Table 1. The CT features of the tumors and thrombi are reported in Table 2.

#### 3.4 | Tumor type prediction

A decision tree method was employed to predict tumor type and the application to our data gave the results illustrated in Figure 2 and presented in Table 3. Because of a lack of a substantial number of adrenocortical adenomas, the analysis was only performed for carcinoma and pheochromocytoma. Thus, as an example, a tumor

**TABLE 1** Mean and median (long-axis dimensions of the tumor and thrombus) dimensions of each tumoral type, with their respective SD and range (minimum-maximum)

	Adenoma	Carcinoma	Pheochromocytoma
Mean ± SD	23 ± 7	28 ± 13	25 ± 11
Short axis dimension (mm)			
Median (min-max)	32 (18-48)	38 (19-110)	38 (19-73)
Long axis dimension (mm)			
Mean ± SD	40 ± 18	35 ± 8 <sup>a</sup>	48 ± 15 <sup>a</sup>
Precontrast attenuation (HU)			
Mean ± SD	96 ± 42	90 ± 27 <sup>b</sup>	115 ± 25 <sup>b</sup>
Postcontrast attenuation (HU)			
Mean ± SD	6 ± 2 <sup>c</sup>	6 ± 2 <sup>d</sup>	7 ± 2 <sup>cd</sup>
Size of contralateral AG (mm)			
Mean ± SD	-	8 ± 4 <sup>e</sup>	15 ± 8 <sup>e</sup>
Short axis of the thrombus (mm)			
Median (min-max)	-	17 (5-38) <sup>f</sup>	44 (6-270) <sup>f</sup>
Long axis of the thrombus (mm)			

Note: The level of significance was set at .05. Superscript of the same letter indicate significant difference between two tumoral types.

Abbreviations: AG, adrenal gland; HU, Hounsfield unit.

	Adenoma	Carcinoma	Pheochromocytoma
<b>The tumor itself</b>			
Heterogeneous enhancement	9	40	29
Presence of a peripheral rim enhancement	4	21	16
Presence of mineral foci within the tumor	4	25 <sup>a</sup>	6 <sup>a</sup>
Irregular contours	3 <sup>bc</sup>	31 <sup>b</sup>	29 <sup>c</sup>
Presence of hyperattenuating adjacent adipose tissue	1	13	13
Evidence of tumor rupture	0	7	4
<b>The thrombus</b>			
Presence of mineral foci within the thrombus	0	6 <sup>e</sup>	3 <sup>e</sup>
Homogeneous enhancement of the thrombus	0	6	10

**TABLE 2** Number of cases observed of selected imaging features for each tumoral type

Note: The level of significance was set at .05. Superscript of the same letter indicate significant difference between two tumoral types.

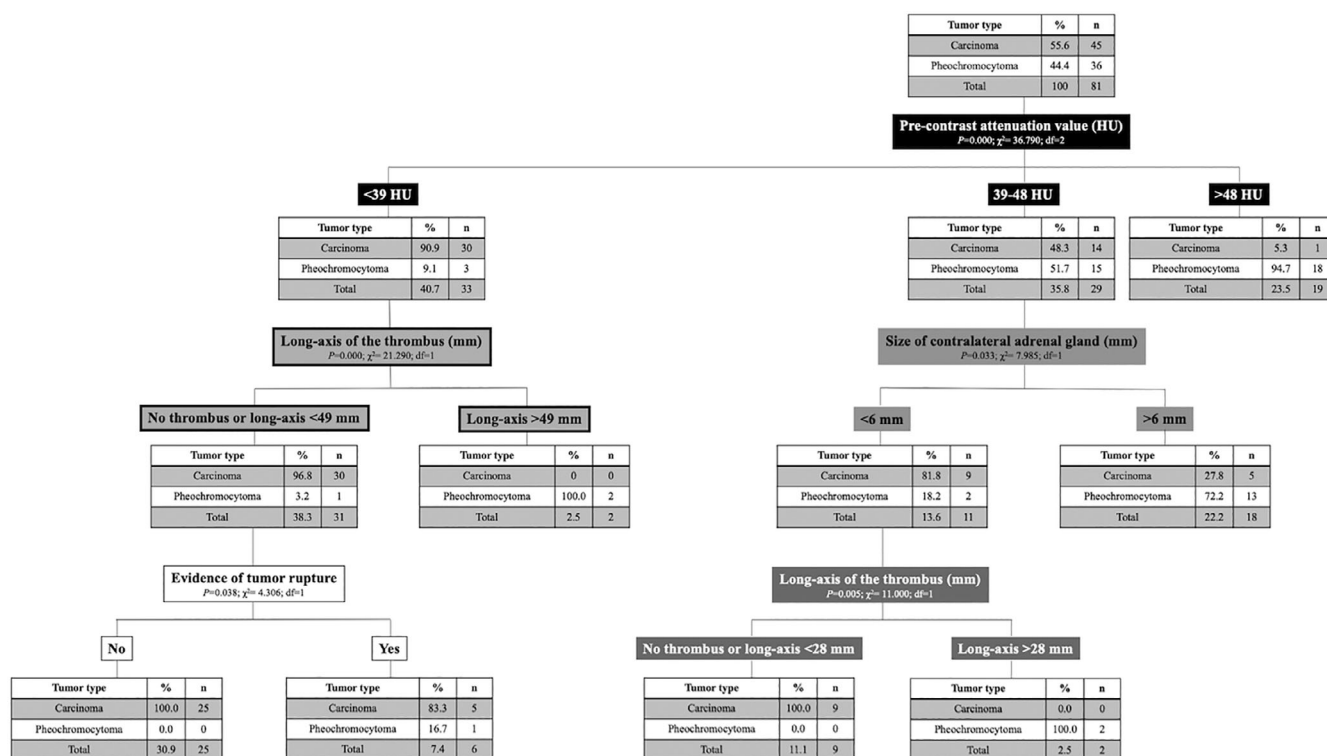


**FIGURE 2** Decision tree obtained based on CT criteria differentiating pheochromocytoma from adrenocortical carcinoma. A tumor demonstrating a precontrast attenuation value <39 HU and a thrombus with a long-axis dimension <49 mm has a probability of 97% to represent a carcinoma and associated with almost 32 times the risk of a wrong diagnosis, that is, pheochromocytoma based on histopathological report. A tumor demonstrating a precontrast attenuation value >48 HU has a probability of 95% to represent a pheochromocytoma. Note the gray zone where the precontrast attenuation value is in between 39 and 48 HU and where the size of the contralateral AG can help discriminate the two types of tumor but with a lesser level of probability (70%-80%) in absence of vascular invasion

demonstrating a precontrast attenuation value <39 HU, with vascular invasion and a thrombus with a long axis dimension <49 mm has a probability of 97% of being an adrenocortical carcinoma and it is associated with almost 32 times the risk of a wrong diagnosis (ie, to be identified as a pheochromocytoma). A tumor with a precontrast attenuation value >48 HU has a 95% probability of being a

pheochromocytoma. An equivocal zone was identified, in which the precontrast attenuation value is between 39 and 48 HU and where the size of the contralateral adrenal gland can help discriminate between the 2 types of tumor, but with a lower level of probability (70%-80%). The CT characteristic features for adrenocortical carcinoma and pheochromocytoma are provided in Figures 3 and 4.



**TABLE 3** Set of rule of thumbs associated with the decision tree

Rule number	Condition 1	Condition 2	Condition 3	Probability CARC	Probability PHEO	ODDS CARC
	No evidence			45%	55%	0.82
1	PCAT $\leq$ 39			91%	9%	10.11
1.1	PCAT $\leq$ 39	LAOT $\leq$ 49		97%	3%	32.33
1.2	PCAT $\leq$ 39	LAOT $>$ 49		0%	100%	-
1.1.1	PCAT $\leq$ 39	LAOT $\leq$ 49	TURU "No"	100%	0%	Inferior
1.1.2	PCAT $\leq$ 39	LAOT $\leq$ 49	TURU "Yes"	83%	17%	4.88
				100%		Inferior
2	$<$ 39 PCAT $\leq$ 48			48%	52%	0.92
2.1	$<$ 39 PCAT $\leq$ 48	SICO $\leq$ 6		82%	18%	4.56
2.2	$<$ 39 PCAT $\leq$ 48	SICO $>$ 6		28%	72%	0.39
2.1.1	$<$ 39 PCAT $\leq$ 48	SICO $\leq$ 6	LAOT $\leq$ 28	100%	0%	Inferior
2.1.2	$<$ 39 PCAT $\leq$ 48	SICO $\leq$ 6	LAOT $>$ 28	0%	100%	-
				48%	52%	0.92
3	PCAT $>$ 48			5%	95%	0.05

Abbreviations: CARC, carcinoma; LAOT, long axis of the thrombus; PCAT, precontrast attenuation; PHEO, pheochromocytoma; SICO, size of contralateral adrenal gland; TURU, tumor rupture.

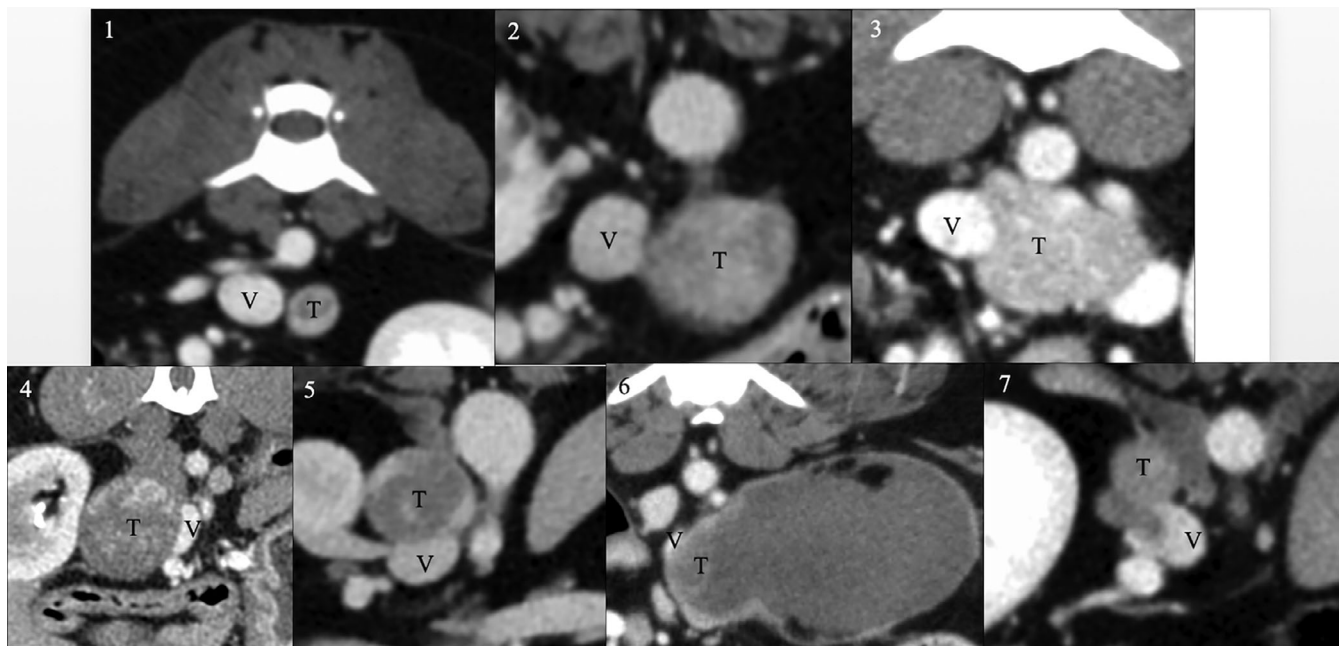


**FIGURE 3** Transverse postcontrast CT images of seven different adrenal tumors (T) illustrating the 7 different scores according to the 7-point scale CT grading system. The vessel is depicted by the letter V. Grade 1 represents an absence of contact between the vessel and the mass as a layer of adipose tissue is identified in between. Grade 2 shows contact between the two structures, affecting less than 90° of the vessel. Grade 3 represents contact affecting more than 90° of the vessel with a concave aspect of the tumor, encircling the vessel. Grade 4 depicts increased contact between the structures, affecting more than 90° of the vessel, with a convex aspect of the tumor against the vessel, the two structures having smooth regular margins. In grade 5, the tumor also has a convex aspect against the vessel; however, the margins are irregular and ill-defined. A grade 6 represents a compression of the vessel by the tumor making it impossible to identify the contact point. Grade 7 describes a clear invasion of the vessel by the tumor

### 3.5 | General performance of the 7-point scale CT grading system

Comparison of the performance of each radiologist with the evaluation of the surgeon (gold standard) for selection of vessels using the

7-point scale CT grading system is depicted in Table 4. For example, the sensitivity in the diagnosis of CVC invasion ranges from 91% to 97% and the specificity between 70% and 86%, depending on the radiologist, with an excellent DOR, ranging from 29 to 141. The sensitivity in the diagnosis of renal vein invasion was less accurate, ranging

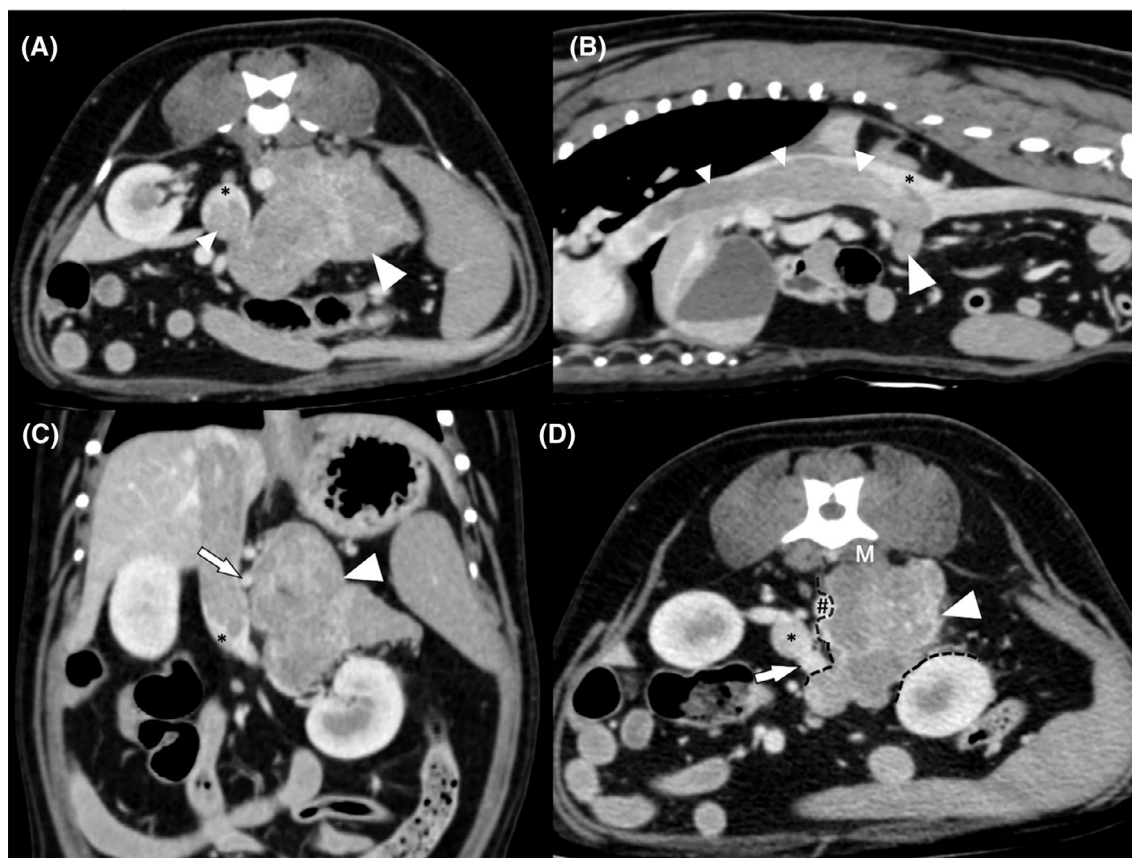


**FIGURE 4** Postcontrast computed tomographic images of a pheochromocytoma invading the left adrenal gland in a 13-year-old Jack Russell Terrier. (A) Transverse postcontrast CT image illustrating the heterogeneously contrast enhancing tumor (white large arrowhead) deforming the contours of the left adrenal gland that is no longer recognizable. A voluminous tumor thrombus (white small arrowhead) is seen invading the caudal vena cava (\*) through the left phrenicoabdominal vein. (B) Sagittal multiplanar reformatted image illustrating the length of the tumor thrombus (small white arrowheads) in the caudal vena cava (\*) and its continuity with the tumor (large white arrowhead). (C) Dorsal multiplanar reformatted image showing the close contact between the tumor (large white arrowhead) and the cranial mesenteric artery (white arrow). Note the contrast enhancement of the tumor thrombus that is similar to the main tumor. (D) Transverse multiplanar reformatted image showing the tumor encircling the abdominal aorta (#) and in close contact with the left renal vein (white arrow) without invading it. The cleavage between the tumor (large white arrowhead) and those structures is depicted by the black dotted line.

from 60% to 88% and the specificity ranged between 14% and 31%, depending on the radiologist, with a fair DOR of 17. Illustration of each grade by CT images is provided in Figure 3.

### 3.6 | Agreement among radiologists using the 7-point scale CT grading system

The agreement among radiologists for each vessel is reported in Table 5. The radiologists' agreement was excellent for the CVC and good to moderate for the other vessels.

### 3.7 | Evaluation of intermediate grades 3, 4, 5, and 6 of the 7-point scale CT grading system and probability of invasion of a given vessel for a given radiologist

Radiologists performed well when there was clear invasion (grade 7) or clear absence of invasion (grades 1 and 2) of the vessels. However,

in the intermediate grades (ie, from 3 to 6 of the 7-point scale CT grading system), corresponding to a level of uncertainty, a marked decrease in the DOR was observed for the 3 radiologists. Bayes' theorem was applied to answer the question "What is the probability of observing invasion in the CVC if only a grade 3 (intermediate, uncertain answer) or a combination of intermediate grades had been formulated by a radiologist?" Table 6 shows the Bayes' posterior probability for each intermediate grade and for each vessel for the radiologist who performed best. Column "3456" is a combined measure and shows the posterior probability if a grade 3, 4, 5, or 6 was given. The probability of observing during surgery invasion into the CVC, the phrenicoabdominal vein or the renal vein was 85%, 84%, and 81%, respectively, if a grade 3, 4, 5, or 6 was given. The probability of observing during surgery an adhesion to the aorta or cranial mesenteric artery was 87% and 88%, respectively, if a grade 3, 4, 5, or 6 was given. Regarding the presence of adhesions with the mesenteric artery or aorta based on presence or absence of visualization of the mesenteric lymphatic tissue and presence or absence of its enhancement, the posterior probability of correct grading (ie, both for



**TABLE 4** Comparison of the performance of each radiologist with the surgery (Golden standard) for a selection of vessels and organs/tissues using the 7-point scale computed tomography grading system

	Rad	Accuracy	Se	Sp	PPV	NPV	TPR	FPR	TNR	FNR	LR+	LR-	DOR	S(DOR)	z	P value
CVC	1	82%	91%	74%	77%	77%	91%	26%	74%	9%	349%	12%	29	0.622	5.414	0.022
	2	81%	97%	70%	70%	79%	97%	30%	70%	3%	323%	4%	86	1.057	4.211	0.021
	3	91%	96%	86%	89%	78%	96%	14%	86%	4%	671%	5%	141	0.846	5.85	0.014
Renal vein	1	88%	97%	31%	89%	29%	97%	69%	31%	3%	141%	8%	17	0.935	3.023	0.047
	2	60%	100%	14%	58%	38%	100%	86%	14%	0%	117%	0%	NA	NA	NA	NA
	3	88%	97%	31%	89%	29%	97%	69%	31%	3%	141%	8%	17	0.935	3.023	0.047
PA vein	1	60%	87%	55%	28%	81%	87%	45%	55%	13%	194%	24%	8	0.794	2.624	0.073
	2	59%	92%	54%	23%	81%	92%	46%	54%	8%	201%	15%	13	1.069	2.41	0.064
	3	58%	91%	54%	21%	81%	91%	46%	54%	9%	197%	17%	12	1.073	2.287	0.071

Note: The variables: Aorta and Cranial Mesenteric artery are not included as not enough positive cases were observed, falsifying the statistical analysis.

Abbreviations: CVC, caudal vena cava; DOR, diagnostic odds ratio = LR+/LR-; FNR, false negative rate; FPR, false positive rate; LR-, negative likelihood ratio = FNR/TNR; LR+, positive likelihood ratio = TPR/FPR; NA, not applicable (index not calculable due to lack of positive or negative assignments (zeros)); NPV, negative predictive value; PA, phrenicoabdominal; PPV, positive predictive value; Rad, radiologist; Se, sensitivity; Sp, specificity; TNR, true negative rate; TPR, true positive rate.

presence and absence of adhesions) is presented in Table 7. The probability of observing adhesions during surgery with the mesenteric artery was 16% when mesenteric lymphatic tissue was observed and 52% when not observed.

### 3.8 | Image quality

The transverse images were judged as the most useful to assess vascular invasion for the CVC and the PA vein. The transverse and dorsal MPR images were the most useful planes to evaluate the renal vein, and transverse and sagittal MPR images were the most relevant for the aorta and cranial mesenteric artery. The median quality of the CT studies evaluated by the 3 radiologists was 4.1/5 (range, 1-5). The main technical limitations of the CT studies with a low grade were the presence of streamlining artifacts mimicking an intracaval filling defect or hampering its correct visualization when present, an insufficient amount of contrast medium, a delayed acquisition after contrast administration, or thick collimation (>2.5 mm) providing inferior MPR images with lack of isotropism. For 35/91 dogs, no arterial acquisition phase had been performed. According to the 3 radiologists, the arterial phase rarely was useful to assess vascular invasion. The main reported advantage of having an arterial phase was better delineation of the tumor margins, improving the visualization of the contact point with adjacent vessels.

## 4 | DISCUSSION

We identified CT features that help the radiologist in predicting the histopathologic type of AT and in providing probability of invasion of adjacent vessels. Preoperative imaging evaluation of AT should include morphology of the tumor,<sup>13,22</sup> its relationship with the adjacent vessels,<sup>5,13</sup> and peri-adrenal extension.

Several tumor characteristics were useful to predict tumor type. As already predicted by other studies, adrenocortical carcinomas seemed to present with lower precontrast CT attenuation values.<sup>13,22</sup> This finding may be because of more parenchymal necrosis associated with this tumoral type<sup>27-29</sup> or more intraparenchymal hemorrhage in pheochromocytomas.<sup>27</sup> Adrenocortical carcinomas also were reported previously to rupture more frequently compared to pheochromocytomas, which was confirmed in our study.<sup>15</sup> Pheochromocytomas also were rarely mineralized, and this finding was also consistent with previous reports.<sup>15,30</sup> Interestingly, we observed longer thrombi associated with pheochromocytoma. Not surprisingly, irregularity of the contours of the tumors also seemed an interesting criterion to predict malignancy because a statistically significant difference was observed between adrenocortical adenomas and carcinomas or metastatic pheochromocytomas. This difference may be explained by the fact that malignant tumors are known to invade the capsule which may be a histopathological criterion to predict malignancy.<sup>27-29</sup>

Integrating several criteria such as the propensity for adrenocortical carcinomas to rupture, to have lower precontrast CT attenuation

**TABLE 5** Table depicting the radiologists' agreement

		ICC single	ICC average	Weighted K	Low CI	High CI
CVC	1 vs 2	0.941	0.97	0.939	0.883	0.995
	2 vs 3	0.912	0.954	0.905	0.821	0.989
	1 vs 3	0.888	0.941	0.887	0.796	0.978
Renal vein	1 vs 2	0.689	0.816	0.613	0.482	0.744
	2 vs 3	0.602	0.752	0.52	0.365	0.675
	1 vs 3	0.62	0.765	0.617	0.459	0.775
PA vein	1 vs 2	0.608	0.756	0.583	0.449	0.717
	2 vs 3	0.502	0.669	0.5	0.332	0.667
	1 vs 3	0.473	0.642	0.443	0.275	0.611
Aorta	1 vs 2	0.737	0.849	0.737	0.576	0.898
	2 vs 3	0.688	0.815	0.682	0.506	0.857
	1 vs 3	0.446	0.617	0.442	0.216	0.668
Cranial mesenteric artery	1 vs 2	0.52	0.684	0.516	0.364	0.667
	2 vs 3	0.663	0.798	0.644	0.499	0.79
	1 vs 3	0.545	0.705	0.541	0.446	0.637
	Agreement		Excellent	Good	Moderate	

Note: Comparisons are made for pairs of radiologists and for each variable. Green color refers to excellent agreement, yellow color, to good agreement and red color, to moderate agreement.

Abbreviations: ICC average, intraclass correlation coefficient between average scores; ICC single, intraclass correlation coefficient between single scores; low CI and high CI, limits of confidence interval at 95%; weighted K, Cohen's K with quadratic weights.

**TABLE 6** Bayes' posterior probability for each intermediate grade (3-6) and for each vessel according to the radiologist 3

Vessel	3	4	5	6	3456
Aorta	85%	74%	100%	100%	87%
Cranial mesenteric artery	90%	77%	87%	100%	88%
Caudal vena cava	57%	100%	78%	100%	85%

Note: Column "3456" show the posterior probability IF a grade 3 OR 4 OR 5 OR 6 is given. For example, the probability to observe surgically an invasion in CVC is 78% if a grade 5 has been assigned; note that 78% is not the relative frequency of right observation of radiologist 3 (grade5), because according with Bayes' theorem, it is weighted by "prior" probability and hence it encompasses and overcome the totally random grading (50%).

Mesenteric lymphatic tissue	Mesenteric artery adhesences	Aortic adhesences
Observed	16%	8%
Not observed	52%	17%
Presence of enhancement	NA	NA
Absence of enhancement	14%	7%

Note: For example, the probability to observe surgically adhesences with the mesenteric artery was 16% when mesenteric lymphatic tissue was observed and 52% when not observed. Abbreviation: NA, not available (not enough cases for reliable calculation).

**TABLE 7** Bayes' posterior probability for identification of adhesences with the mesenteric artery and aorta based on presence or absence of visualization of the mesenteric lymphatic tissue and presence or absence of its enhancement according to the radiologist 3

value and present with a shorter tumor thrombus, a decision tree was developed. This probabilistic method can help the radiologist in differentiating adrenocortical carcinomas and pheochromocytomas, in the absence or presence of laboratory and clinical information, which is crucial information for the internist, anesthetist and surgeon involved in therapeutic planning.<sup>7,22</sup> Unfortunately, adrenocortical adenomas had to be excluded because only 9 cases were present in the study population, and including them in the

probabilistic tree would have decreased the discriminatory power of the algorithm.

We based our algorithm on precontrast CT attenuation values obtained from AT tissue. This choice was made because the study was a multicenter study with different protocols of administration of contrast medium. The dose of contrast medium and the timing of postinjection CT scanning are known to be the main determinants of peak attenuation for the adrenal gland in healthy dogs.<sup>31</sup> Therefore,

comparing the postcontrast CT value of ATs as a variable among tumor types was considered as not reliable because there were too many variations related to protocols of injection and dose. Another finding was the smaller than expected lesser discriminatory power of contralateral adrenal size in the decision tree. Smaller diameter is expected in functional cortisol-secreting carcinomas because of negative feedback.<sup>32</sup> The presence of contralateral adrenal gland >6 mm in the carcinoma group could be related to a hormonally silent adrenocortical tumor or because of concurrent pituitary and adrenocortical lesions.<sup>33</sup> These findings also corresponded to the category that was more difficult to discriminate from pheochromocytoma regarding tumor type. In this equivocal situation, ultrasound-guided fine needle aspiration of the AT may be considered because it is known as a safe technique<sup>34,35</sup> and cytological analysis can allow good discrimination between neuroendocrine and epithelial origin of the tumor.<sup>36</sup>

We used a decision tree method to analyze our data. The main difference compared to other approaches (eg, logit models) is the capacity of decision trees to identify a threshold in continuous variables (eg, attenuation or axis of thrombus) under and over which the probability of identifying the kind of tumor becomes significantly lower or higher compared to the alternative diagnosis. In addition, it is possible to weigh the risk of misclassification with a cost function representing the (probabilistic) gain or loss associated with a wrong decision (ie, type I and type II statistical errors). The most useful output of a decision tree is a sequence of rules (type IF, THEN) that can minimize the risk-cost function. A negative aspect of this method was that the branches of the tree used different criteria in a particular order, so that not every criterion might be used in a particular case. For instance, on the right side, rupture was not used. The readers of this decision tree should avoid any confusion using this approach in the clinic when they have criteria that they have not used to make a decision.

In our study, excellent agreement among radiologists and excellent performance (high accuracy and DOR) were observed when using the 7-point scale CT grading system of the CVC in dogs with ATs. This finding is in agreement with previous studies in which high sensitivity and specificity in the detection of vascular invasion in the CVC were demonstrated in CT.<sup>15,16</sup> However, in these studies, there was no description of the CT interpretation technique, no evaluation of the repeatability of the method and no evaluation of the performance of the CT in predicting invasion of other important vessels such as the cranial mesenteric artery, aorta, renal and PA veins. Moreover, those studies used a binary system (ie, presence or absence of vascular invasion) which in our opinion does not reflect the clinical situation.

In our study, agreement among radiologists was moderate to good for invasion of the renal and PA veins, and the performance of the 7-point scale CT grading system compared to surgery was modest. It is unclear whether this result is because surgeons may not have documented sufficient detail in their surgical reports regarding potential invasion of those vessels or they may have had difficulty appreciating the relationship between the mass and these vessels because of poor visualization through large fat deposits or hemorrhage. It also may be a consequence of the small size of these vessels and thus

greater difficulty in their evaluation by the radiologists, or because an equivocal zone exists between 3 and 6 in the CT grading system, making the diagnosis of vascular invasion for those vessels not possible with CT. However, a probability of invasion still could be provided by the radiologist to the surgeon and internist, when an intermediate grade (3-6) is given for a vessel, to improve surgical planning. This is particularly important for the CVC, renal vein, aorta, and mesenteric artery. When a tumor involves the left adrenal gland, it is crucial for the surgeon to know if adherence to the aorta and cranial mesenteric artery is present. While retracting the mesentery and small intestine to the right to access the left adrenal gland, the surgeon loses visualization of the point of contact between the tumor and those vessels, making dissection between the 2 very critical. Any perforation during surgery of the cranial mesenteric artery or aorta could lead to fatal hemorrhage. For grade 3 and above, there is a high risk (>85%) that adhesion is present between the tumor and the aorta or cranial mesenteric artery. A prospective study is needed to further characterize the CT appearance of adherence and vascular wall invasion.

Evaluation of the mesenteric lymphatic tissue did not provide any relevant and consistent information regarding the probability of adherence. Therefore, the results of our study suggested that evaluation of the presence or absence and enhancement of this tissue was not indicated in the evaluation of the presence of adherence with arterial vessels. Although this network does not drain the adrenal gland (lumbo-aortic network), we thought that contiguity with the lymphatic tissue could explain potential local invasion by the tumor. This hypothesis was not confirmed in our study.

The radiologist's interpretation of the CT scan plays an important role in the presurgical planning for dogs with AT. However, it can be difficult for the radiologist to know which criteria and information are most relevant for the surgeon. The aim of the 7-point scale CT grading system is to allow better communication between the surgeon and the radiologist so that all of the essential information necessary for the surgeon may be evaluated by the radiologist.

Sagittal and dorsal MPR were chosen by the radiologists in the study as the most useful and relevant planes for the evaluation of potential invasion and contact point between the tumor and the aorta, cranial mesenteric and renal vein, respectively. However, MPR were of limited value when the slice thickness, pitch, or both were too high, and caused a stair-step artifact, partial volume artifact and a high pitch blurring. This latter artifact is the result of the nonplanar geometry of helical image data requiring interpolation into planar image data sets. These artifacts are a hindrance to evaluate vascular anatomy and may explain the difficulty for the radiologists to assess vascular invasion of vessels such as the PA, renal veins, and cranial mesenteric artery. A logistic regression model could have been performed, with image quality measures such as slice thickness or voxel size and diagnostic accuracy or probability as variables to assess whether the poor image quality correlated with decreased accuracy.

Other important variables that had impact on the quality of the CT studies and on the evaluation of vascular invasion were related to contrast distribution and quantity. The presence of streamlining artifact, with insufficient amount of contrast medium used or too much

delay in acquisition of the postcontrast series, contributed to decreased image quality. Streamlining artifacts would create an image of pseudo-thrombus because of heterogeneous filling of the vascular lumen, possibly contributing to misinterpretation and resulting in radiologist error. Insufficient amount of contrast medium or too great a delay in acquisition of the postcontrast series were considered as having a negative impact on the visualization of tumor thrombus because of the lack of intravascular contrast and sufficient enhancement to delineate the contours of the thrombus. The effects of contrast medium injection technique on attenuation values of the adrenal glands in healthy dogs during contrast-enhanced CT has been studied,<sup>31</sup> but no study has evaluated the effects of injection protocol on the attenuation of adjacent vessels and intravascular contrast distribution.

Mortality and survival time unfortunately were not evaluated in our study and therefore no correlation between the extent of vascular invasion or compression and survival time was performed for these patients.

Although the CT features have been detailed in our study, no information on the patients' signalment, endocrine activity of the ATs or description of the histopathological findings have been evaluated and integrated. Clinical and laboratory findings represent the first step in the diagnostic evaluation of dogs with ATs. These factors do have an impact on the decision tree and were not considered in our study. Radiologists using this decision tree should consider clinical and laboratory findings, when available, and integrate them into their decision process.

Another limitation of our study is the lack of clarity on the diagnostic criteria for histopathological diagnosis, especially for pheochromocytoma. We had decided to rely on histopathological reports of each institution and use them as the gold standard. However, discrepancies among laboratories may exist, especially if different criteria are used, and between old and more recent cases, as new classifications have been established.

The last limitation of our study was related to the complexity of the CT grading system which may limit its feasibility in clinical practice. However, it was designed to improve communication among internists, surgeons, and radiologists, to provide probabilities of vascular invasion, and to express the difficulty in establishing a distinction between invasion or no invasion.

## 5 | CONCLUSION

A decision tree using the variables of precontrast attenuation value of the AT, the long axis of the thrombus, the presence of tumor rupture and the size of the contralateral adrenal gland was proposed to assist the radiologist in the differentiation among tumor types. Using a 7-point scale CT grading system, the radiologist can provide information on the probability of invasion of adjacent vessels by an AT to the internist, surgeon, and anesthetist.

## ACKNOWLEDGMENT

No funding was received for this study. The authors thank Wladimir Peltzer for the illustrations, and all the radiologists and veterinarians

that have indirectly participated in the collection of cases, in particular Simone Perfetti, Manuela Quinci, and Isabella Guarnera.

## CONFLICT OF INTEREST DECLARATION

Authors declare no conflict of interest.

## OFF-LABEL ANTIMICROBIAL DECLARATION

Authors declare no off-label use of antimicrobials.

## INSTITUTIONAL ANIMAL CARE AND USE COMMITTEE (IACUC) OR OTHER APPROVAL DECLARATION

Authors declare no IACUC or other approval was needed.

## HUMAN ETHICS APPROVAL DECLARATION

Authors declare human ethics approval was not needed for this study.

## ORCID

Pascaline Pey  <https://orcid.org/0000-0003-3917-4756>

Alessia Diana  <https://orcid.org/0000-0003-1709-3920>

Federico Fracassi  <https://orcid.org/0000-0003-3121-2199>

## REFERENCES

- Lunn KF, Boston SE. Tumors of the endocrine system. In: Withrow SJ, Vail DM, eds. *Withrow & MacEwen's Small Animal Clinical Oncology*. 6th ed. St. Louis: Saunders Elsevier; 2020:565-596.
- Behrend EN. Non-cortisol-secreting adrenocortical tumors and incidentalomas. In: Ettinger SJ, Feldman EC, eds. *Textbook of Veterinary Internal Medicine*. 8th ed. St. Louis: Elsevier; 2017:1819-1825.
- Galac S. Pheochromocytoma. In: Ettinger SJ, Feldman EC, eds. *Textbook of Veterinary Internal Medicine*. 8th ed. St. Louis: Elsevier; 2017: 1838-1843.
- Gilson SD, Withrow SJ, Orton EC. Surgical treatment of pheochromocytoma: technique, complications, and results in six dogs. *Vet Surg*. 1994;23(3):195-200.
- Kyles AE, Feldman EC, De Cock HEV, et al. Surgical management of adrenal gland tumors with and without associated tumor thrombi in dogs: 40 cases (1994-2001). *J Am Vet Med Assoc*. 2003;223:654-662.
- Barrera JS, Bernard F, Ehrhart EJ, Withrow SJ, Monnet E. Evaluation of risk factors for outcome associated with adrenal glands tumors with or without invasion of the caudal vena cava and treated via adrenalectomy in dogs: 86 dogs (1993-2009). *J Am Vet Med Assoc*. 2013; 242:1715-1721.
- Herrera M, Mehl M, Kass P, et al. Predictive factors and the effect of phenoxybenzamine on outcome in dogs undergoing adrenalectomy for pheochromocytoma. *J Vet Intern Med*. 2008;22:1333-1339.
- Schwartz P, Kovak JR, Koprowski A, Ludwig LL, Monette S, Bergman PJ. Evaluation of prognostic factors in the surgical treatment of adrenal gland tumors in dogs: 41 cases (1999-2005). *J Am Vet Med Assoc*. 2008;232:77-84.
- Lang JM, Schertel E, Kennedy S, Wilson D, Barnhart M, Danielson B. Elective and emergency surgical management of adrenal gland tumors: 60 cases (1999-2006). *J Am Anim Hosp Assoc*. 2011;47: 428-435.
- Massari F, Nicoli S, Romanelli G, Buracco P, Zini E. Adrenalectomy in dogs with adrenal gland tumors: 52 cases (2002-2008). *J Am Vet Med Assoc*. 2011;239:216-221.
- Mayhew PD, Boston SE, Zwingenberger AL, et al. Perioperative morbidity and mortality in dogs with invasive adrenal neoplasms treated by adrenalectomy and cavotomy. *Vet Surg*. 2019;48(5): 742-750.

12. Cavalcanti JVJ, Skinner OT, Mayhew PD, Colee JC, Boston SE. Outcome in dogs undergoing adrenalectomy for small adrenal gland tumours without vascular invasion. *Vet Comp Oncol.* 2020;18(4):599-606.
13. Mayhew PD, Culp WTN, Balsa IM, Zwingenberger AL. Phrenicoabdominal venotomy for tumor thrombectomy in dogs with adrenal neoplasia and suspected vena caval invasion. *Vet Surg.* 2018;47:227-235.
14. Knight R, Lamb C, Brockman DJ, Lipscomb VJ. Variations in surgical technique for adrenalectomy with caudal vena cava venotomy in 19 dogs. *Vet Surg.* 2019;48:751-759.
15. Schultz RM, Wisner ER, Johnson EG, MacLeod JS. Contrast-enhanced computed tomography as a preoperative indicator of vascular invasion from adrenal masses in dogs. *Vet Radiol Ultrasound.* 2009;50:625-629.
16. Gregori T, Mantis P, Benigni L, Priestnall SL, Lamb CR. Comparison of computed tomographic and pathologic findings in 17 dogs with primary adrenal neoplasia. *Vet Radiol Ultrasound.* 2015;56:153-159.
17. Morandi F. Adrenal glands. In: Schwarz T, Saunders J, eds. *Veterinary Computed Tomography.* Chichester, West Sussex, UK: John Wiley & Sons; 2011:351-356.
18. Wisner E, Zwingenberger AL. Adrenal glands. In: Wisner E, Zwingenberger AL, eds. *Atlas of Small Animal CT and MRI.* 1st ed. Ames, Iowa, USA: John Wiley & Sons; 2015:561-571.
19. Bertolini G. MDCT of hyperadrenocorticism. In: Bertolini G, ed. *Body MDCT in Small Animals: Basic Principles, Technology, and Clinical Applications.* 1st ed. New York, NY: Springer Berlin Heidelberg; 2017:393-406.
20. Zaky AM, Wolfgang CL, Weiss MJ, Javed AA, Fishman EK, Zaheer A. Tumor-vessel relationships in pancreatic ductal adenocarcinoma at multidetector CT: different classification systems and their influence on treatment planning. *Radiographics.* 2017;37:93-112.
21. Zhang L, Zhang ZY, Ni JM, et al. Prediction of vascular invasion using a 3-point scale computed tomography grading system in pancreatic ductal adenocarcinoma: correlation with surgery. *J Comput Assist Tomogr.* 2017;41:394-400.
22. Reusch C, Feldman E. Canine hyperadrenocorticism due to adrenocortical neoplasia. Pretreatment evaluation of 41 dogs. *J Vet Intern Med.* 1991;5:3-10.
23. Perfetti S, Diana A, Baron Toaldo M, Cipone M, Quinci M, Pey P. CT measures of adrenal gland length and caudal pole diameter are reproducible in large breed dogs: a pilot study. *Vet Radiol Ultrasound.* 2021;62:402-412. doi:10.1111/vru.12970
24. R-project.org [Internet]. Vienna, Austria: A Language and Environment for Statistical Computing. R Foundation for Statistical Computing. <http://www.R-project.org/>. Accessed 25 October 2021.
25. Hastie T, Tibshirani R, Friedman J. *Elements of Statistical Learning.* 2nd ed. New York, USA: Springer; 2013.
26. Sheng L, Ni Z. Cost-sensitive test strategies. AAAI'06: *Proceedings of the 21st National Conference on Artificial Intelligence.* Vol 1; New York, USA: ACM Digital Library; 2006:482-487.
27. Kiupel M, Capen C, Miller MR, Smedley. *Histological Classification of Tumors of the Endocrine System of Domestic Animals.* Vol 12. Washington, DC: Armed Forces Institute of Pathology—World Health Organization; 2008.
28. Labelle P, Kyles AE, Farver TB, de Cock HEV. Indicators of malignancy of canine adrenocortical tumors: histopathology and proliferation index. *Vet Pathol.* 2004;41(5):490-497.
29. Sanders K, Cirkel K, Grinwis GCM, et al. The Utrecht score: a novel histopathological scoring system to assess the prognosis of dogs with cortisol-secreting adrenocortical tumours. *Vet Comp Oncol.* 2019;17(3):329-337.
30. Yoshida O, Kutara K, Seki M, et al. Preoperative differential diagnosis of canine adrenal tumors using triple-phase helical computed tomography: preoperative CT of canine adrenal tumors. *Vet Surg.* 2016;45:427-435.
31. Blaser A, Drenner M, Mosing M, et al. Effects of contrast medium injection technique on attenuation values of adrenal glands in healthy dogs during contrast-enhanced computed tomography. *Am J Vet Res.* 2016;77:144-150.
32. Rodríguez Piñeiro MI, de Fornel-Thibaud P, Benchekroun G, et al. Use of computed tomography adrenal gland measurement for differentiating ACTH dependence from ACTH independence in 64 dogs with hyperadrenocorticism. *J Vet Intern Med.* 2011;25:1066-1074.
33. van Bokhorst KL, Kooistra HS, Boroffka SAEB, Galac S. Concurrent pituitary and adrenocortical lesions on computed tomography imaging in dogs with spontaneous hypercortisolism. *J Vet Intern Med.* 2019;33:72-78.
34. Sumner J, Lacorcía L, Rose A, et al. Clinical safety of percutaneous ultrasound-guided fine-needle aspiration of adrenal gland lesions in 19 dogs. *J Small Anim Pract.* 2018;59:357-363.
35. Pey P, Diana A, Rossi F, et al. Safety of percutaneous ultrasound-guided fine-needle aspiration of adrenal lesions in dogs: perception of the procedure by radiologists and presentation of 50 cases. *J Vet Intern Med.* 2020;34(2):626-635.
36. Bertazzolo W, Didier M, Gelain M, et al. Accuracy of cytology in distinguishing adrenocortical tumors from pheochromocytoma in companion animals. *Vet Clin Pathol.* 2014;43:453-459.

**How to cite this article:** Pey P, Specchi S, Rossi F, et al. Prediction of vascular invasion using a 7-point scale computed tomography grading system in adrenal tumors in dogs. *J Vet Intern Med.* 2022;36(2):713-725. doi:10.1111/jvim.16371